

# Green-emitting $\text{CaF}_2:\text{Ce}^{3+}, \text{Tb}^{3+}$ phosphor: selection for improving luminous flux and color quality of conformal geometry white LED lamps

PHU TRAN TIN<sup>1</sup>, TRAN HOANG QUANG MINH<sup>2,\*</sup>, NGUYEN HUU KHANH NHAN<sup>2</sup>, HSIAO-YI LEE<sup>2</sup>, TRAN THANH TRANG<sup>3</sup>

<sup>1</sup>Faculty of Electronics Technology, Industrial University of Ho Chi Minh City, Ho Chi Minh City, Vietnam

<sup>2</sup>Optoelectronics Research Group, Faculty of Electrical and Electronics Engineering, Ton Duc Thang University, Ho Chi Minh City, Vietnam

<sup>3</sup>Faculty of Electrical and Electronics Engineering, Ho Chi Minh City University of Food Industry, 140 Le Trong Tan, Ho Chi Minh City, Vietnam

In the last decades, new solutions for improving lighting properties of white LED lamps (WLEDs) have been the main research direction in optoelectronics. In this paper, a modern approach for enhancing luminous flux and color quality of white LED lamps was presented. By mixing green-emitting  $\text{CaF}_2:\text{Ce}^{3+}, \text{Tb}^{3+}$  phosphor with yellow-emitting YAG:Ce phosphor compound, the luminous flux and color quality of white LED lamps with conformal phosphor geometry (CPG) increased significantly. From the obtained results it follows that, the luminous flux increased more than 1.5 times, and the correlated color temperature deviation decreased more than 4 times in comparison with the non-green-emitting  $\text{CaF}_2:\text{Ce}^{3+}, \text{Tb}^{3+}$  phosphor. The presented research shows that the green-emitting  $\text{CaF}_2:\text{Ce}^{3+}, \text{Tb}^{3+}$  phosphor could become a good candidate for enhancing luminous flux and color quality of white LED lamps.

Keywords: white LED lamps (WLEDs); conformal phosphor geometry; green-emitting  $\text{CaF}_2:\text{Ce}^{3+}, \text{Tb}^{3+}$  phosphor; luminous flux; color quality

## 1. Introduction

Due to their significant advantages (high efficiency, long lifetime, compactness, low cost, high color quality, and reliability), white LED lamps (WLEDs) have been considered as very important lighting devices. Since their invention to date, WLEDs have been produced by several methods. Firstly, WLEDs were fabricated by a combination of blue, green and red light chips to emit white light spectrum. However, the high manufacturing cost and the required complicated electronics were disadvantages of this approach. Another method has been coating of some yellow emitting phosphor, like  $\text{Y}_3\text{Al}_5\text{O}_{12}:\text{Ce}^{3+}$  (YAG:Ce), on blue LED phosphors, which resulted in white light emission. However, YAG:Ce WLEDs have

a low color rendering index (CRI) and high correlated color temperature deviation (D-CCT). Therefore, it was difficult to use them for indoor lighting applications. The third approach is a combination of multiple phosphor materials coated on a LED chip, known as PC-LEDs. The luminescence of PC-LEDs is significantly influenced by packing, assembly of phosphors, and strong re-absorption of blue light by green and red phosphors. The third approach is commonly used in research and manufacturing of WLEDs. In recent years, many studies have focused on enhancement of lighting performance of W-LEDs packages by the third approach [1, 2].  $\text{SiO}_2$  added to YAG:Ce phosphor improved its color quality [3]. D-CCT and CRI of WLEDs were enhanced by doping  $\text{Y}_2\text{O}_3:\text{Eu}^{3+}$  to YAG:Ce phosphor [4, 5]. To improve color uniformity, WLEDs containing  $\text{Y}_2\text{O}_3:\text{Eu}^{3+}$  phosphor and green Ce, Tb phosphor were produced. However,

\*E-mail: tranhoangquangminh@tdtu.edu.vn

these studies only focused on increasing color uniformity and did not pay much attention to the enhancement of both luminous flux and color quality of the WLEDs. A gap has remained, which could be filled by this research work.

Hollow micro- and nanostructures with their unique properties, such as low density, high surface-to-volume ratio, low coefficient of thermal expansion, and low refractive index, have been applied in drug-delivery carriers, efficient catalysis, sensors, active-material encapsulation, photonic crystals, etc. [6, 7]. Microstructured solid fluoride materials, due to their properties (low-energy phonons, high ionicity, electron-acceptor behavior, high resistivity, and anionic conductivity), have been used in optical applications. Among them, calcium fluoride ( $\text{CaF}_2$ ) with low refractive index and wide band gap is widely applied in optoelectronic devices. Moreover, calcium fluoride ( $\text{CaF}_2$ ) is well-known as the host for luminescent ions ( $\text{Ce}^{3+}$  and  $\text{Tb}^{3+}$ ) due to its high transparency in a broad wavelength range, low refractive index, and low phonon energy as shown in [8, 9]. Due to its significant advantages, green-emitting  $\text{CaF}_2:\text{Ce}^{3+},\text{Tb}^{3+}$  phosphor can be considered as a prospective solution in WLEDs lighting [10]. Nevertheless, there have been only few studies, which demonstrated green-emitting  $\text{CaF}_2:\text{Ce}^{3+},\text{Tb}^{3+}$  phosphor for enhancing the luminous flux and color quantity of RP-WLEDs yet.

In this research, a new approach consisting in mixing green-emitting  $\text{CaF}_2:\text{Ce}^{3+},\text{Tb}^{3+}$  particles into a YAG:Ce phosphor compound of white LED lamps with conformal phosphor geometry (CPG) to improve their luminous flux and color quantity (CRI, CQS, D-CCT) was proposed. The influence of both size and concentration of green-emitting  $\text{CaF}_2:\text{Ce}^{3+},\text{Tb}^{3+}$  particles on the lighting performance was analyzed and investigated.

This paper can be divided into three parts. In the first part, a physical simulation model of WLEDs using a Light Tools software is presented. After that, the influence of both size and concentration of green-emitting  $\text{CaF}_2:\text{Ce}^{3+},\text{Tb}^{3+}$  particles is evaluated and analyzed by the commercial Light Tools software and MATLAB. In this part,

the size of green-emitting  $\text{CaF}_2:\text{Ce}^{3+},\text{Tb}^{3+}$  particles is changed from 1  $\mu\text{m}$  to 10  $\mu\text{m}$ , and its concentration is varied from 0 % to 30 % for non-green-emitting  $\text{CaF}_2:\text{Ce}^{3+},\text{Tb}^{3+}$  particles. Finally, some results are demonstrated and discussed. It is shown that in green-emitting  $\text{CaF}_2:\text{Ce}^{3+},\text{Tb}^{3+}$  phosphor, luminous flux increased more than 1.5 times, and the correlated color temperature deviation decreased more than 4 times in comparison with the non-green-emitting  $\text{CaF}_2:\text{Ce}^{3+},\text{Tb}^{3+}$  phosphor. Consequently, the green-emitting  $\text{CaF}_2:\text{Ce}^{3+},\text{Tb}^{3+}$  phosphor can be considered as a new solution for enhancing the luminous flux and color quality of white LED lamps.

## 2. Physical model and mathematical description

The real WLED with 9 LED chips has been used to simulate the physical model using the commercial Light Tools 8.1.0 software (Fig. 1). The Light Tools 8.1.0 is based on the Monte Carlo ray-tracing method. The real WLED has the following parameters:

1. Each LED chip with a 1.14 mm square base and a 0.15 mm height is bonded with a reflector. The power of each blue chip is 1.16 W.
2. The reflector has an 8 mm bottom length, a 2.07 mm height, and a 9.85 mm length.
3. The conformal phosphor coating which covers the nine chips, has a fixed thickness of 0.08 mm.

The refractive indexes of the green-emitting  $\text{CaF}_2:\text{Ce}^{3+},\text{Tb}^{3+}$  and YAG:Ce phosphors are 1.52 and 1.83, respectively. The refractive index of the silicone glue is 1.5. The dopping particles density has been varied to fix the average CCT value. If the weight percentage of the green-emitting  $\text{CaF}_2:\text{Ce}^{3+},\text{Tb}^{3+}$  particles is increased, the weight of YAG:Ce phosphor needs to be reduced to maintain the average CCT value.

Mathematical description is given by Mie theory [11–13]. The scattering coefficient  $\mu_{\text{sca}}(\lambda)$ ,

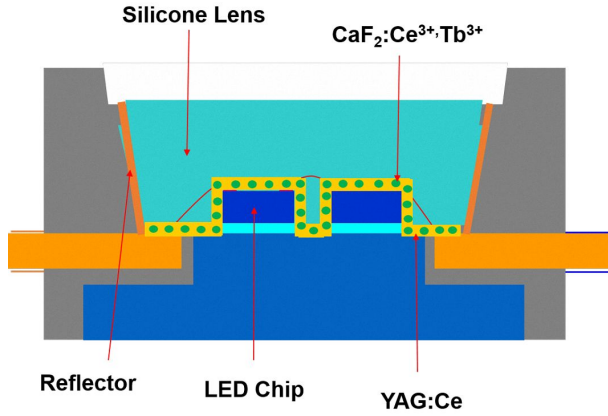


Fig. 1. Physical structure of conformal phosphor geometry (CPG) W-LED.

anisotropy factor  $g(\lambda)$ , and reduced scattering coefficient  $\delta_{sca}(\lambda)$  can be computed by expression 1, expression 2, and expression 3, respectively:

$$\mu_{sca}(\lambda) = \int N(r)C_{sca}(\lambda, r)dr \quad (1)$$

$$g(\lambda) = 2\pi \int_{-1}^1 p(\theta, \lambda, r)f(r) \cos \theta d \cos \theta dr \quad (2)$$

$$\delta_{sca} = \mu_{sca}(1 - g) \quad (3)$$

where  $N(r)$  is the density distribution of diffusion particles in  $\text{mm}^3$ ,  $C_{sca}$  is the scattering cross section in  $\text{mm}^2$ ,  $p(\theta, \lambda, r)$  is the phase function,  $\lambda$  is the light wavelength in nm,  $r$  is the radius of diffusional particles in  $\mu\text{m}$ ,  $\theta$  is the scattering angle in  $^\circ$ ,  $f(r)$  is the size distribution function of the green-emitting  $\text{CaF}_2:\text{Ce}^{3+}, \text{Tb}^{3+}$  particles, which can be obtained by equation 4 and equation 5:

$$f(r) = f_{dif}(r) + f_{phos}(r) \quad (4)$$

$$\begin{aligned} N(r) &= N_{dif}(r) + N_{phos}(r) \\ &= K_N \cdot [f_{dif}(r) + f_{phos}(r)] \end{aligned} \quad (5)$$

$N(r)$  is composed of diffusive particle number density  $N_{dif}(r)$  and the phosphor particle number density  $N_{phos}(r)$ ,  $f_{dif}(r)$  and  $f_{phos}(r)$  are the size distribution functions of the diffuser and phosphor particle.

Here,  $K_N$  is the number of unit diffuser for one diffuser concentration and can be calculated by:

$$c = K_N \int M(r)dr \quad (6)$$

where  $M(r)$  is the mass distribution of the unit diffuser expressed by the equation:

$$M(r) = \frac{4}{3} \pi r^3 [\rho_{dif} f_{dif}(r) + \rho_{phos} f_{phos}(r)] \quad (7)$$

$\rho_{dif}(r)$  and  $\rho_{phos}(r)$  are the density of diffuser and phosphor crystal.

In Mie theory,  $C_{sca}$  can be calculated by the following expression:

$$C_{sca} = \frac{2\pi}{k^2} \sum_0^\infty (2n-1)(|a_n|^2 + |b_n|^2) \quad (8)$$

where  $k = 2\pi/\lambda$ , and  $a_n$  and  $b_n$  are calculated by:

$$a_n(x, m) = \frac{\psi'_n(mx)\psi_n(x) - m\psi_n(mx)\psi'_n(x)}{\psi'_n(mx)\xi_n(x) - m\psi_n(mx)\xi'_n(x)} \quad (9)$$

$$b_n(x, m) = \frac{m\psi'_n(mx)\psi_n(x) - \psi_n(mx)\psi'_n(x)}{m\psi'_n(mx)\xi_n(x) - \psi_n(mx)\xi'_n(x)} \quad (10)$$

where  $x = k \cdot r$ ,  $m$  is the refractive index, and  $\psi_n(x)$  and  $\xi_n(x)$  are the Riccati-Bessel functions.

In RP-WLEDs, the refractive index of silicone  $n_{sil}$  is 1.53.  $n_{dif}$  is the refractive index of diffuser.  $n_{phos}$  is the refractive index of phosphor particle. Therefore, the relative refractive indices of diffuser  $m_{dif}$  and phosphor  $m_{phos}$  in the silicone can be calculated by  $m_{dif} = n_{dif}/n_{sil}$  and  $m_{phos} = n_{phos}/n_{sil}$ . Then, the phase function  $p(\theta, \lambda, r)$  can be expressed by:

$$p(\theta, \lambda, r) = \frac{4\pi\beta(\theta, \lambda, r)}{k^2 C_{sca}(\lambda, r)} \quad (11)$$

where  $\beta(\theta, \lambda, r)$ ,  $S_1(\theta)$  and  $S_2(\theta)$  are calculated by the following equations:

$$\beta(\theta, \lambda, r) = \frac{1}{2} [|S_1(\theta)|^2 + |S_2(\theta)|^2] \quad (12)$$

$$\begin{aligned} S_1 &= \sum_{n=1}^\infty \frac{2n+1}{n(n+1)} [a_n(x, m)\pi_n(\cos\theta) \\ &\quad + b_n(x, m)\tau_n(\cos\theta)] \end{aligned} \quad (13)$$

$$S_2 = \sum_{n=1}^{\infty} \frac{2n+1}{n(n+1)} [a_n(x, m)\tau_n(\cos\theta) + b_n(x, m)\pi_n(\cos\theta)] \quad (14)$$

In equation 13 and equation 14,  $\tau_n(\cos\theta)$  and  $\pi_n(\cos\theta)$  are angular dependent functions.

### 3. Results and discussion

In this research, the coefficients were calculated by MATLAB software using Mie theory. In computing of Mie-scattering, the concentration of  $\text{CaF}_2:\text{Ce}^{3+}, \text{Tb}^{3+}$  particles is varied from 0 % to 30 %, continuously. In Fig. 2, the scattering coefficients grow with the growing concentration of  $\text{CaF}_2:\text{Ce}^{3+}, \text{Tb}^{3+}$ . The scattering coefficients take higher values at 555 nm and lower ones at 680 nm. In this situation, the yellow light intensity becomes stronger in comparison with the red light intensity, which results in decreasing of various intensity distributions between yellow and red light. In addition, the participation of  $\text{CaF}_2:\text{Ce}^{3+}, \text{Tb}^{3+}$  particles enhances the absorption ability of yellow light and the main purpose of  $\text{CaF}_2:\text{Ce}^{3+}, \text{Tb}^{3+}$  particles is to compensate red light in WLEDs. From these reasons,  $\text{CaF}_2:\text{Ce}^{3+}, \text{Tb}^{3+}$  could be used for improving color quality and luminous flux of WLEDs. Fig. 3 shows the anisotropy factors of  $\text{CaF}_2:\text{Ce}^{3+}, \text{Tb}^{3+}$  particles for wavelengths of 453 nm, 555 nm, and 680 nm, respectively. The results indicate that the anisotropy factor values at 555 nm wavelength are higher than those at 680 nm and 453 nm. It means that  $\text{CaF}_2:\text{Ce}^{3+}, \text{Tb}^{3+}$  should display a stronger scattering at 555 nm. The computed results have been adjusted by Monte Carlo simulation. The anisotropy factors show a slight deviation ranging from 0.916 to 0.927, which results in an insignificant scattering effect regardless of wavelength. It could be beneficial for the color quality of WLEDs. However, the reduced coefficient is almost the same for 680 nm, 555 nm, and 453 nm wavelengths (Fig. 4). The reduced scattering coefficients of  $\text{CaF}_2:\text{Ce}^{3+}, \text{Tb}^{3+}$  for 453 nm, 555 nm, and 680 nm wavelengths grow with  $\text{CaF}_2:\text{Ce}^{3+}, \text{Tb}^{3+}$  concentration. The deviations of the reduced scattering coefficients for these three wavelengths are very small.

The results demonstrate that  $\text{CaF}_2:\text{Ce}^{3+}, \text{Tb}^{3+}$  has a significant influence on scattering, anisotropy, and reduced coefficients (Fig. 5).

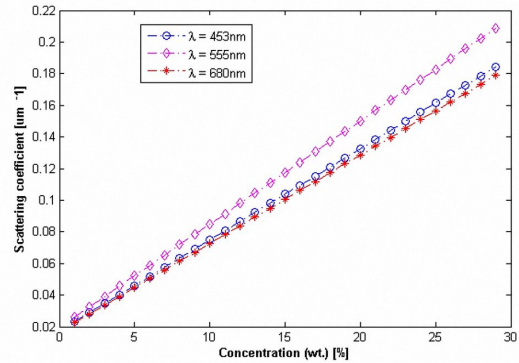


Fig. 2. Scattering coefficients of  $\text{CaF}_2:\text{Ce}^{3+}, \text{Tb}^{3+}$  at wavelengths of 453 nm, 555 nm, and 680 nm.

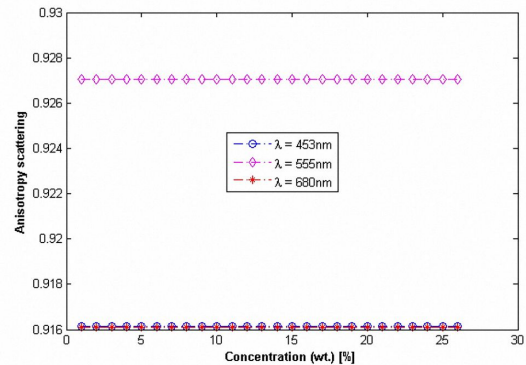


Fig. 3. Anisotropy scattering of  $\text{CaF}_2:\text{Ce}^{3+}, \text{Tb}^{3+}$  at wavelengths of 453 nm, 555 nm, and 680 nm.

Using the commercial Light Tool software, the CRI, CQS, CCT deviations, and lumen output of WLEDs with  $\text{CaF}_2:\text{Ce}^{3+}, \text{Tb}^{3+}$  particles have been calculated. As shown in Fig. 6 and Fig. 7, D-CCT values of 7000 K and 8500 K WLEDs decrease more than 4 times. These results could be explained by compensating red light in PC-LED as a result of employing  $\text{CaF}_2:\text{Ce}^{3+}, \text{Tb}^{3+}$  particles phosphor. The minimum D-CCT has been obtained for 1  $\mu\text{m}$  in size and 12 % concentration of  $\text{CaF}_2:\text{Ce}^{3+}, \text{Tb}^{3+}$  particles. The higher concentration and less size of  $\text{CaF}_2:\text{Ce}^{3+}, \text{Tb}^{3+}$  particles, the smaller D-CCT value. On the other hand, the luminous flux values

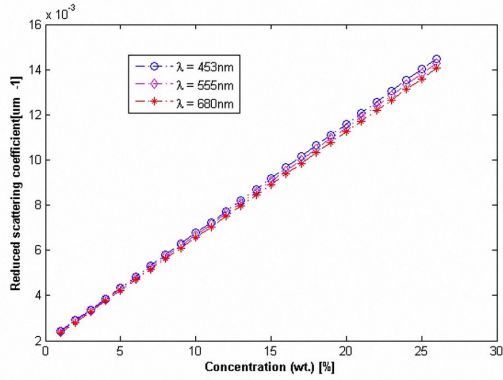


Fig. 4. Reduced scattering coefficient of  $\text{CaF}_2:\text{Ce}^{3+}, \text{Tb}^{3+}$  at wavelengths of 453 nm, 555 nm, and 680 nm.

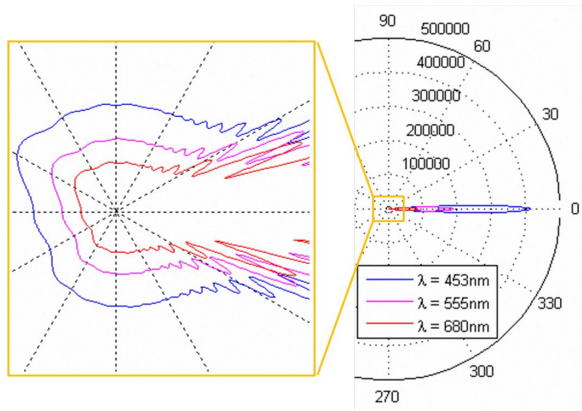


Fig. 5. Angular scattering amplitudes of  $\text{CaF}_2:\text{Ce}^{3+}, \text{Tb}^{3+}$  at wavelengths of 453 nm, 555 nm and 680 nm.

of 7000 K and 8500 K WLEDs increase significantly with increasing concentration and decreasing size of  $\text{CaF}_2:\text{Ce}^{3+}, \text{Tb}^{3+}$  particles. The luminous flux may increase by more than 1.5 times (Fig. 12 and Fig. 13). The maximum value of luminous flux is near 950 Lm for 1  $\mu\text{m}$  size and 12 % concentration of  $\text{CaF}_2:\text{Ce}^{3+}, \text{Tb}^{3+}$  particles. However, the CRI and CQS show a slight decrease with increasing concentration and decreasing size of  $\text{CaF}_2:\text{Ce}^{3+}, \text{Tb}^{3+}$  particles (Fig. 8, Fig. 9, Fig. 10, and Fig. 11). This results could be explained by the enhanced scattering effect of yellow light in phosphor compound when adding  $\text{CaF}_2:\text{Ce}^{3+}, \text{Tb}^{3+}$  particles. From these results, it can be inferred that the optimal size and concentration of  $\text{CaF}_2:\text{Ce}^{3+}, \text{Tb}^{3+}$  particles are 1  $\mu\text{m}$  and 12 %, respectively. Finally,

the results show that both the size and concentration of  $\text{CaF}_2:\text{Ce}^{3+}, \text{Tb}^{3+}$  particles have a significant influence on the color quality and luminous efficiency of WLEDs.

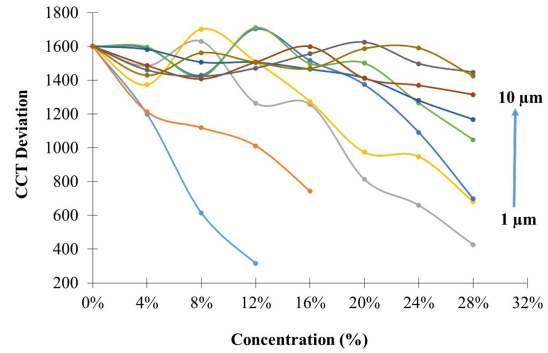


Fig. 6.  $\Delta\text{CCT}$  deviation of W-LEDs 7000 K at different percentages of green-emitting  $\text{CaF}_2:\text{Ce}^{3+}, \text{Tb}^{3+}$  phosphor particles.

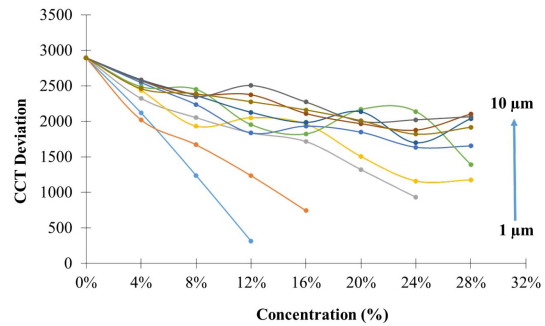


Fig. 7.  $\Delta\text{CCT}$  deviation of W-LEDs 8500 K at different percentages of green-emitting  $\text{CaF}_2:\text{Ce}^{3+}, \text{Tb}^{3+}$  phosphor particles.

## 4. Conclusions

In this research, the influence of the green-emitting  $\text{CaF}_2:\text{Ce}^{3+}, \text{Tb}^{3+}$  phosphor on luminous flux and color quality of white LED lamps with conformal phosphor geometry has been demonstrated. From simulation results and theory analysis, some conclusions are proposed:

1. Luminous flux of white LED lamps is influenced by the size

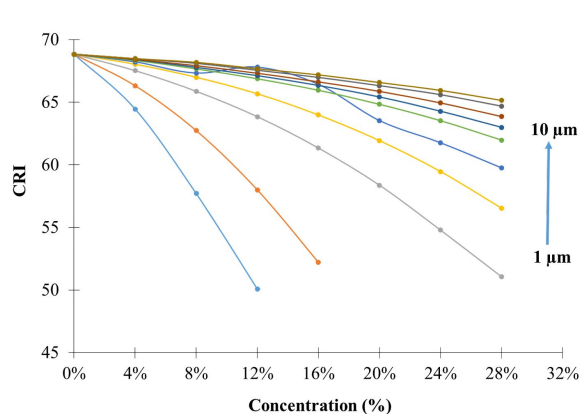


Fig. 8. CRI of W-LEDs 7000 K at different percentages of green-emitting  $\text{CaF}_2:\text{Ce}^{3+}, \text{Tb}^{3+}$  phosphor particles.

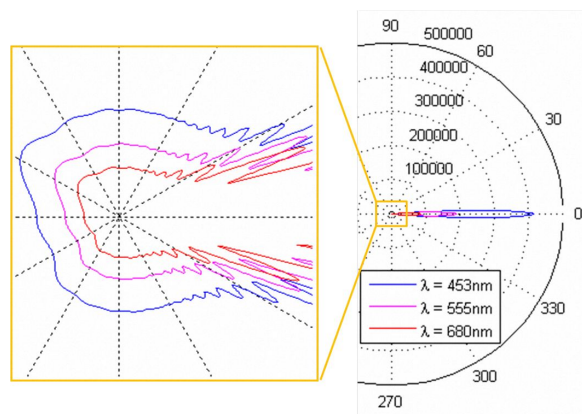


Fig. 11. CQS properties of W-LEDs 8500 K at different percentages of green-emitting  $\text{CaF}_2:\text{Ce}^{3+}, \text{Tb}^{3+}$  phosphor particles.

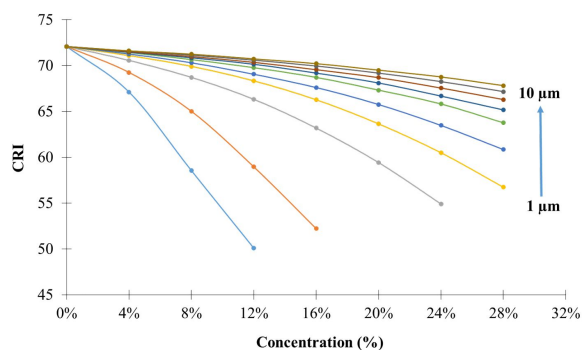


Fig. 9. CRI of W-LEDs 8500 K at different percentages of green-emitting  $\text{CaF}_2:\text{Ce}^{3+}, \text{Tb}^{3+}$  phosphor particles.

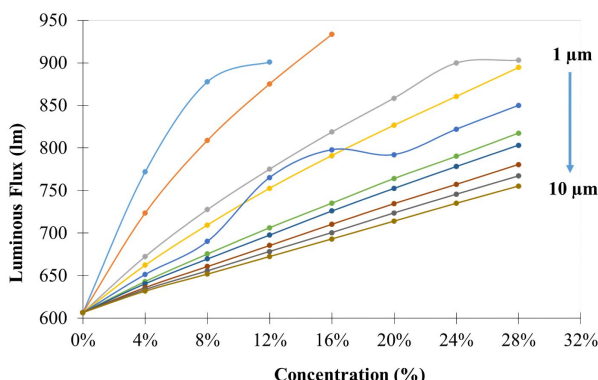


Fig. 12. Luminous flux of W-LEDs 7000 K at different percentages of green-emitting  $\text{CaF}_2:\text{Ce}^{3+}, \text{Tb}^{3+}$  phosphor particles.

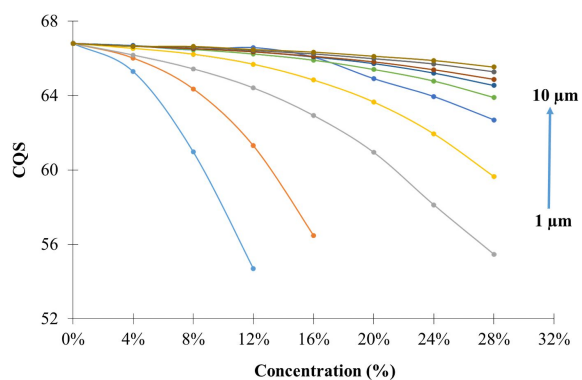


Fig. 10. CQS properties of W-LEDs 7000 K at different percentages of green-emitting  $\text{CaF}_2:\text{Ce}^{3+}, \text{Tb}^{3+}$  phosphor particles.

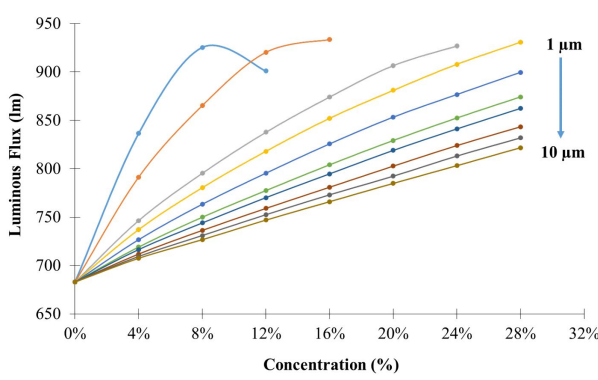


Fig. 13. Luminous flux of W-LEDs 8500 K at different percentages of green-emitting  $\text{CaF}_2:\text{Ce}^{3+}, \text{Tb}^{3+}$  phosphor particles.

and concentration of green-emitting  $\text{CaF}_2:\text{Ce}^{3+},\text{Tb}^{3+}$  phosphor. Luminous flux increased about 1.5 times when adding green-emitting  $\text{CaF}_2:\text{Ce}^{3+},\text{Tb}^{3+}$  phosphor to the phosphor compound.

2. CCT deviation decreased more than 4 times with varying concentration and size of green-emitting  $\text{CaF}_2:\text{Ce}^{3+},\text{Tb}^{3+}$  phosphor.
3. CRI and CQS of the white LED lamps slightly decreased when the concentration and size of green-emitting  $\text{CaF}_2:\text{Ce}^{3+},\text{Tb}^{3+}$  phosphor continuously increased.

This study provides critical approach to using green-emitting  $\text{CaF}_2:\text{Ce}^{3+},\text{Tb}^{3+}$  phosphor for W-LEDs applications. In further work, the influence of the green-emitting  $\text{CaF}_2:\text{Ce}^{3+},\text{Tb}^{3+}$  phosphor on luminous flux and color quality of in-cup and remote packaged W-LEDs will be presented and analyzed.

## References

- [1] ANH N.D.Q., LAI M.F., MA H.Y., LEE H.Y., *J. Chin. Inst. Eng.*, 38 (2014), 297.
- [2] LAI M.F., ANH N.D.Q., MA H.Y., LEE H.Y., *J. Chin. Inst. Eng.*, 39 (2016), 468.
- [3] LIU S., LUO X., *LED Packaging for Lighting Applications*, Wiley, Beijing, 2011.
- [4] ANH N.D.Q., LEE H.Y., *J. Chin. Inst. Eng.*, 39 (2016), 871.
- [5] MINH T.H.Q., NHAN N.H.K., VO T.P., ANH N.D.Q., *Adv. Electr. Electron. Eng.*, 14 (2016), 340.
- [6] KWAK J., LIM J., PARK M., LEE S., CHAR K., LEE C., *Nano Lett.*, 15 (2015), 3793.
- [7] ADUSUMALLI V.N.K.B., HERAMBA V.S.R.M., MAHALINGAM V., *J. Mater. Chem. C*, 4 (2016), 2289.
- [8] ZHANG C., LI C., PENG C., CHAI R., HUANG S., YANG D., CHENG Z., LIN J., *Chem.-Eur. J.*, 16 (2010), 5672.
- [9] CHEN T.M., YANG Y.J., *Phosphors, Up Conversion Nano Particles, Quantum Dots and Their Applications*, Springer, 2016.
- [10] AMSTER R.L., *J. Electrochem. Soc.*, 117 (1970), 791.
- [11] ZHONG J., XIE M., OU Z., ZHANG R., HUANG M., ZHAO F., *Sym. Photonics Optoelectron.*, (2011), 878.
- [12] YEN W., WEBER M., *Inorganic Phosphors*, CRC Press, London, 2004.
- [13] SCHUBERT E.F., *Light-Emitting Diodes*, Cambridge University Press, London, 2006.

Received 2017-02-10

Accepted 2018-05-05